A Conserved Major Groove Antideterminant for *Saccharomyces cerevisiae* RNase III Recognition†

Mui Sam, Anthony K. Henras, and Guillaume Chanfreau*

Department of Chemistry and Biochemistry and Molecular Biology Institute, Box 951569, University of California, Los Angeles, California 90095-1569

Received November 30, 2004; Revised Manuscript Received January 10, 2005

ABSTRACT: Rnt1p, the only known *Saccharomyces cerevisiae* RNase III double-stranded RNA endonuclease, plays important roles in the processing of precursors of ribosomal RNAs and small nuclear and nucleolar RNAs and in the surveillance of unspliced pre-mRNAs. Specificity of cleavage by Rnt1p relies on the presence of RNA tetraloop structures with the consensus sequence AGNN at the top of the target dsRNA. The sequences of 79 fungal RNase III substrates were inspected to identify additional conserved sequence elements or antideterminants that may contribute to Rnt1p recognition of the double-stranded RNA. Surprisingly, U-A sequences at the base pair adjacent to the conserved terminal tetraloop (closing base pair) were found to be absent from all but one inspected sequence. Analysis of chemically modified variants of the closing base pair showed that the presence of exocyclic groups in the major groove of purines 3′ to the last nucleotide of the tetraloop inhibits Rnt1p cleavage without strongly inhibiting Rnt1p binding. We propose that these groups interfere with the recognition of the RNA substrate by the catalytic domain of Rnt1p. These results identify exocyclic groups of purines in the major groove downstream of the tetraloop as a major antideterminant in *S. cerevisiae* RNase III activity, and suggest a rationale for their apparent counter selection in RNA processing sites.

Double-stranded RNA endonucleases from the RNase[1] III family participate in the processing of a large number of stable RNAs. Eukaryotic RNase III-like proteins are involved in the maturation of the precursor of rRNAs (*1*−*3*), and in the RNA interference and microRNA processing pathways (*4*−*8*). Eukaryotic RNases III also play important roles in the processing of other stable small RNAs. In *Saccharomyces cerevisiae*, the U1, U2, U4, and U5 snRNAs are processed at their 3′-end by Rnt1p cleavage, followed by exonucleolytic digestion (*9*−*12*). Rnt1p also plays a major function in the 5′-end processing of independently transcribed snoRNAs, as well as in the processing of polycistronic snoRNA precursors (*13*−*15*). The identification of a large number of RNase III processing signals in rRNA, snRNA, and snoRNA precursors has revealed the presence in the RNA substrate of terminal tetraloops carrying the weak consensus sequence RGNN (*13*, *16*, *17*). These tetraloops are required for efficient Rnt1p cleavage (*16*, *18*). Rnt1p selects the scissile phosphodiester bond 14−16 bp from the RGNN tetraloop, showing that the enzyme acts as an RNA helical ruler (*16*). Determination of the structure of these tetraloops by NMR spectroscopy showed that they adopt a specific conformation in the absence of Rnt1p (*19*, *20*). The most conserved residue, the universal G2, adopts a syn conformation, and the turn of the loop occurs after this universal nucleotide (*19*, *20*). Hydroxyl radical footprinting showed that Rnt1p directly binds the tetraloop region (*21*). The tridimensional shape of these tetraloops, rather than the conserved AG dinucleotide sequence, is recognized by the double-stranded RNA binding domain of Rnt1p (*22*), which can discriminate AGNN-capped dsRNAs from other types of dsRNAs independent of the remainder of the protein (*18*). Surprisingly, the specificity of the dsRBD for the tetraloop relies only on the recognition of the minor groove side of the tetraloop and of the nonconserved bases (*22*). Whether additional domains of the protein also contribute to the specificity of RNA recognition and cleavage is unknown.

While AGNN tetraloops are essential for Rnt1p recognition and cleavage site selection, it seems likely that other determinants of specificity may exist in the RNA substrate. A recent study showed that mutation of some sequences in the vicinity of the tetraloops or near the cleavage site inhibited Rnt1p binding and/or cleavage (*23*). However, it is not clear whether these results can be extrapolated to most Rnt1p substrates, because the results obtained are clearly not correlated to a strong conservation in the sequence phylogeny of the substrates. In this work, we have analyzed the sequences of 79 substrates of RNase III orthologues in closely related yeast species. This analysis revealed that U-A base pairs are almost never found at the immediate basis of the terminal AGNN tetraloop. We will refer in this study to the term "closing base pair" to describe this particular position. We show that the U-A exclusion at the closing base pair position reflects a functional significance, and that these

† This work was supported by an NSF GK-12 Fellowship (M.S.), by a Human Frontier Science Program Organization Postdoctoral Fellowship (A.K.H.), and by National Institute of General Medical Sciences Grant R01 GM-61518 from the National Institutes of Health to G.C.

* To whom correspondence should be addressed. Telephone: (310) 825-4399. Fax: (310) 206-4038. E-mail: guillom@chem.ucla.edu.

[1] Abbreviations: RNase, ribonuclease; dsRNA, double-stranded RNA; rRNA, ribosomal RNA; snRNA, small nuclear RNA; snoRNA, small nucleolar RNA.

10.1021/bi047483u CCC: $30.25
Published on Web 02/19/2005

sequences are excluded from Rnt1p substrates because of the presence of the exocyclic group in the adenine major groove, which interferes with Rnt1p recognition. These results identify a conserved antideterminant for fungal RNases III recognition.

MATERIALS AND METHODS

Sequence Analysis. The sequences of 79 Rnt1p or *Hemiascomycetes* RNase III cleavage sites were compiled from refs *14*, *16*, and *17*. The frequencies of nucleotides at the third and fourth positions of the tetraloop and of base pairs at the first, second, and third positions downstream from the tetraloop were determined by visual inspection of the predicted secondary structures, as determined using Mfold (*24*).

In Vitro Cleavage and Determination of Kinetic Parameters. RNA substrates were chemically synthesized by Dharmacon. In vitro cleavage of 5′-end-labeled substrates using purified recombinant His6-Rnt1p was performed as described previously (*16*). Cleavage reactions were carried out in duplicate under single-turnover conditions with ~0.3 nM RNA and ~37 nM Rnt1p. Time points were taken from 10 s to 120 min, and the products were resolved on a 10% denaturing acrylamide/bisacrylamide (19:1)−0.5× TBE gel. The amount of cleaved product relative to full-length substrate was measured using ImageQuant 5.2. Data were plotted to produce time course traces, which were then fitted to hyperbolic equations. The percentage of uncleaved substrate was then extrapolated from the best-fit curves. To calculate the initial rates of the cleavage reactions, the time points from the first 2 min were fitted to straight lines. The slopes of the lines were designated as the initial rates. Values were reported as the average of two independent experiments. In the case of the C-G, U-A, and U-2AP substrates, similar V_i quantitative differences between these substrates were obtained at 120 nM Rnt1p (data not shown).

Binding Assays. Electrophoretic mobility shift assays (EMSAs) were performed as described previously (*16*), with the following modifications. Binding reactions were initiated at 4 °C in 50 mM Tris-HCl (pH 7.4), 200 mM KCl, 2.5 mM EDTA (pH 8.0), 5 mM spermidine, 0.5 mM DTT, 20% glycerol, and 100 ng/μL BSA. Reaction mixtures were incubated for 20 min on ice and then immediately loaded onto a 4% acrylamide/bisacrylamide (80:1)−50 mM Tris-glycine gel. Gels were run at 6 mA for 5 h at 4 °C. ImageQuant 5.2 was used to quantitate the relative amount of complex formed to free substrate. A plot of the percentage of the bound substrate versus Rnt1p concentration was generated, and the binding constant (K_d) was interpolated from a best-fit hyperbolic curve.

RNase Probing. RNase T1 cleavage was performed as described previously (*16*). RNase A cleavage was performed at room temperature for 6 min in 10 mM Tris-HCl (pH 7.6), 200 mM KCl, 10 mM $MgCl_2$, and 0.1 μg/μL BSA with 0.5−1 ng of RNase A. Cleavage products were resolved on 10% denaturing acrylamide/bisacrylamide (19:1)−0.5× TBE sequencing gels. RNase A accessibility for the closing base pair pyrimidine was calculated by dividing the signal from band a (closing base pair, Figure 4) by the signal from band b (internal cleavage in the stem). Each ratio was then divided by the ratio calculated for the wild-type C-G sequence. The location of RNase A cleavage sites was deduced from relative migration compared to size markers and other RNases cleavage sites (T1).

Table 1: Sequence Analysis of 79 *Hemiascomycetes* RNase III Substrates[a]

loop 3	loop 4	base pair 1	base pair 2	base pair 3
A, 12	A, 25	A-U, 18	A-U, 22	A-U, 31
C, 5	C, 9	C-G, 43	C-G, 13	C-G, 7
G, 30	G, 7	G-C, 14	G-C, 10	G-C, 21
U, 32	U, 38	U-A, 1	U-A, 33	U-A, 13
		U·G, 3	U·G, 1	A-C, 3
				C·U, 1
				G·U, 3

[a] Loop 3 is third position of the tetraloop. Loop 4 is the fourth position of the tetraloop. Base pairs 1−3 represent the first, second, and third base pairs following the AGNN tetraloop, respectively. The number of each nucleotide or base pair observed among a population of 79 substrates is given.

RESULTS

U-A Closing Base Pairs Are Counterselected in Yeast RNase III Substrates. The recent identification of *S. cerevisiae* Rnt1p snoRNA substrates (*14*), as well as the computational screening of homologous target sites in closely related *Hemiascomycetes* species (*17*), led us to revisit the sequences of Rnt1p targets, to identify some sequence (anti)-determinants for RNase III recognition. For *Hemiascomycetes* species closely related to *S. cerevisiae*, the existence of cleavage sites was deduced from their proximity to rRNA and sn(o)RNA sequences and the presence of AGNN-type tetraloops at the tip of the double-stranded RNA structures (*17*). Because the exact location of these cleavage sites was not experimentally mapped, we restricted our sequence analysis to tetraloop sequences and to the first three base pairs localized immediately downstream from the terminal tetraloops. Comparison of the tetraloop sequences revealed that cytosines were under-represented at the third and fourth positions of the tetraloop, and that guanosines were under-represented at the fourth position (loops 3 and 4 in Table 1). AGCC tetraloops were never found among the substrates, possibly because they interfere with formation of the AGNN-type fold (*19*, *20*). When the sequences of the base pairs immediately following the tetraloop (closing base pair) were examined, we noticed that U-A base pairs were absent in all but one of the Rnt1p substrates that were analyzed (Table 1), *RPL18A*. This under-representation of U-A base pairs is probably not due to the lower stability of U-A base pairs compared to G-C or C-G base pairs, as A-U base pairs were encountered frequently (Table 1). In addition, the under-representation of U-A base pairs was unlikely to be specifically due to the presence of a uridine residue, as U·G base pairs are present in three substrates. We therefore suspected that the reason for the under-representation of U-A base pairs was that adenosines located immediately downstream of the last position of the tetraloop might be deleterious to Rnt1p recognition. Inspection of the sequences of the second base pairs downstream from the tetraloops did not reveal any strong sequence conservation or antideterminant, except that G·U base pairs were not found, and only one U·G base pair was found, suggesting a counter selection for wobble base pairs at the penultimate base pair position (Table 1). Analysis of sequences of the third base pairs showed an absence of

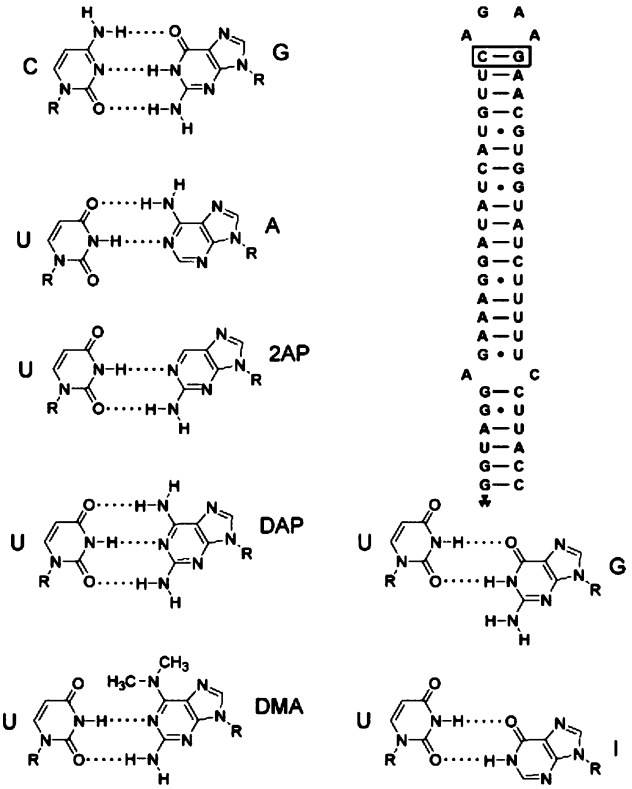

FIGURE 1: Structures of base analogues and corresponding closing base pairs used in this study. The secondary structure of the model substrate derived from the snR47 substrate used in this study is shown, with the closing base pair boxed. Predicted base pair geometries of the variants that have been analyzed are indicated.

U·G base pairs, and showed that C-G base pairs were underrepresented (Table 1).

Overall, the most striking observation that could be made from the inspection of this large number of *Hemiascomycetes* RNase III target sites was the almost complete absence of U-A base pairs closing the tetraloops. We decided to investigate biochemically the significance of this phylogenetic observation.

Exocyclic Groups in the Major Groove of Adenine Derivatives Downstream of the AGNN Tetraloop Inhibit Rnt1p Cleavage Activity. The counter selection of U-A closing base pairs suggested that some element of the adenine base downstream from the tetraloop might be deleterious to Rnt1p binding and/or cleavage, or to the formation of the tetraloop structure. Since guanine bases can be frequently found at this position in the context of C-G base pairs, we suspected that the counterselected element might be the exocyclic N6 amino group (Figure 1). This amino group may be counterselected because it sterically interferes with an element of Rnt1p that interacts with the major groove side of the RNA duplex close to the tetraloop. To understand the basis of the counterselection of U-A closing base pairs, we synthesized various RNA substrates derived from the snR47 model hairpin substrate, whose sequence or structure varies at the closing base pair position (Figure 1). These variants are named according to the nature of the base pair closing the terminal AGAA tetraloop (boxed in Figure 1). Because A-U and G-C base pairs are present at similar frequencies (Table 1), we restricted our biochemical analysis to closing base pairs with a 5′-pyrimidine−3′-purine combination. In addition to C-G (also termed the wild-type) and U-A sequences, we obtained derivatives of U-A base pairs in which the adenine base is modified into a 2-aminopurine (U-2AP), 2,6-diaminopurine (U-DAP), or dimethyladenine (U-DMA) (Figure 1). These derivatives were chosen because they are predicted to form base pairs that are isosteric with U-A and C-G base pairs with respect to the sugar−phosphate backbone position (Figure 1), but they differ by the presence or absence of exocyclic groups in the major groove side of the adenine base. While U-2AP does not present any exocyclic group in the major groove side of the adenine base, U-DAP shows the same exocyclic group as a U-A base pair, and U-DMA presents a much bulkier exocyclic group in the major groove with the presence of two methyl groups (Figure 1). In addition, we also investigated substrates containing a U·G or U·I closing base pair (Figure 1). Although these base pairs are of the wobble type, and therefore not isosteric to the previously described base pairs with respect to the sugar−phosphate backbone position (Figure 1), we decided to investigate their effect on Rnt1p recognition.

These substrates were submitted to in vitro cleavage using purified recombinant Rnt1p in single-turnover kinetics (Figure 2). The U-A mutant was cleaved at a significantly slower rate (4 times slower) than the wild-type C-G construct (Figure 2 and Table 2), correlating with the counterselection of this type of base pair in the substrate phylogeny (Table 1). Strikingly, this initial velocity defect was suppressed by a 3-fold factor in the U-2AP substrate. This suppression effect was also observed on the fraction of unreacted substrate, which is higher for the U-A than for the U-2AP substrate (Figure 2 and Table 2). This result strongly suggests that the defect observed for the U-A substrate is due to the presence of the exocyclic N6 amino group in the major groove of the U-A base pair. Shifting this amino group to position 2 of the purine base eliminates the steric interference in the major groove, while maintaining the hydrogen bond pattern necessary for base pair formation, and restores a cleavage activity close to that of the wild-type.

The U·G mutant exhibited a more pronounced cleavage defect than the U-A sequence (Figure 2 and Table 2). The defects observed for the U·G variant could be explained by the replacement of a Watson−Crick base pair with a wobble base pair. A wobble base pair may be inhibitory to the positioning of the dsRBD. First, wobble base pairs downstream from the tetraloops are relatively rare in the population of substrates that were analyzed (Table 1). In addition, it has been shown that the Rnt1p dsRBD binds the terminal tetraloop and the closing base pair from the minor groove side of the RNA duplex (*22*). Therefore, the shift of the position of the sugar−phosphate backbone toward the minor groove side in a U·G wobble base pair (Figure 1) may interfere with the dsRBD recognition, possibly because the exocyclic guanine amino group in the minor groove interferes with positioning of the dsRBD. This hypothesis is consistent with a partial suppression of the cleavage defect observed with the U·G substrate when the guanosine is replaced with inosine (Figure 2 and Table 2). The U·I variant shows the same wobble geometry and two hydrogen bonds as the U·G base pair (Figure 1), but the exocyclic minor groove amino group is absent. Strikingly, this single shift in the position of the amino group resulted in a 3-fold higher initial velocity than the U·G variant (Table 2).

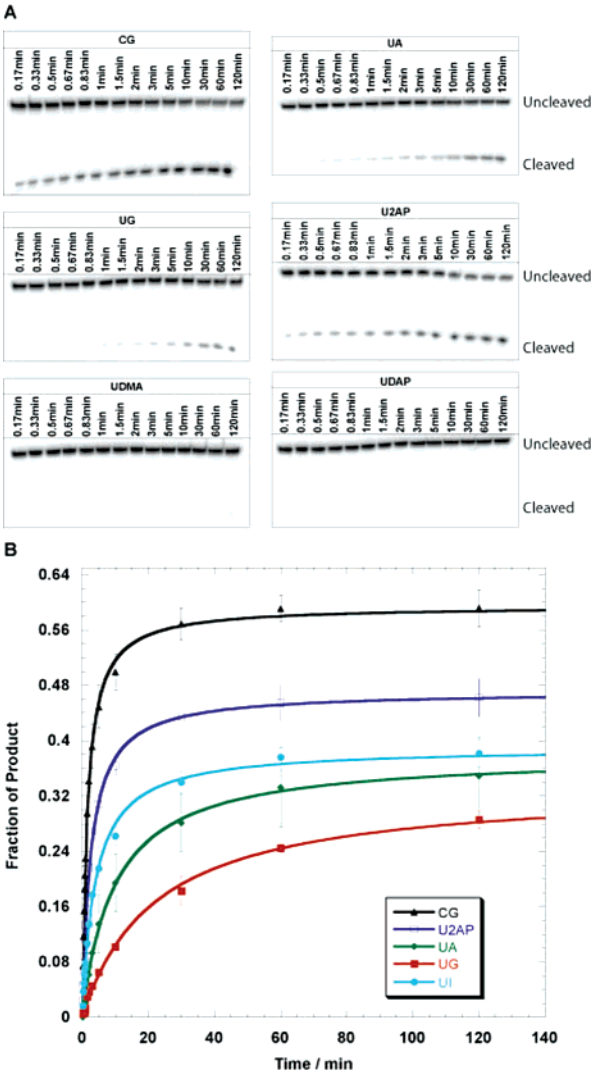

FIGURE 2: Single-turnover kinetics of cleavage of wild-type and modified substrates by recombinant Rnt1p. (A) Polyacrylamide gels of in vitro cleavage time course experiments using 5′-end-labeled substrates. (B) Time course kinetics for the C-G, U-A, U-2AP, U·G, and U·I variants. Because of their apparent lack of reactivity (see panel A), the kinetics are not shown for the U-DMA and U-DAP substrates. Error bars represent variations obtained in two independent experiments. Curves represent the best-fit model.

Substrates with a U-DMA or a U-DAP showed an apparent absence of reactivity (Figure 2A and Table 2). Therefore, their time course is not plotted in Figure 2B. In the case of the U-DAP, this may be due to the presence of the exocyclic N6 amino group in the major groove, but it is likely that other factors contribute as well, since the U-A mutant is not as dramatically perturbed. In the case of the U-DMA, the presence of two bulky methyl groups in the major groove may perturb the positioning of an element of the enzyme in the major groove side, or indirectly perturb the fold of the terminal tetraloop by prohibiting formation of the terminal base pair (see below).

Closing Base Pair Variants Do Not Strongly Inhibit Rnt1p Binding. To try to correlate the results observed in single-turnover kinetics with defects in binding of these substrates by Rnt1p, we monitored the direct binding of Rnt1p to these substrates uncoupled from cleavage with an electrophoretic mobility shift assay (EMSA). Binding of Rnt1p uncoupled from cleavage can be detected by an EMSA in a buffer lacking divalent cations that are necessary for cleavage (*16*, *26*). Interestingly, none of the closing base pair variants exhibited a strong binding defect (Figure 3 and Table 2). In particular, the U-DMA or U-DAP mutants, which were completely unreactive in vitro, had a binding constant only modestly increased compared to that of the C-G wild-type sequence (Table 2). Strikingly, the binding constants of U-A and U-DMA were identical, while their cleavage behavior is dramatically different. The binding constant determined for the U·G substrate was within the margin of error of the constant observed for the wild-type C-G sequence, while the initial velocity of the U·G substrate is 10 times lower than that of the C-G substrate (Table 2). Overall, these results show that the binding of these variants by Rnt1p does not correlate with their cleavage behavior. Thus, it is unlikely that a binding defect is responsible for the inhibitory effect induced by the U-A, U-DMA, and U-DAP variants during the in vitro cleavage reaction using purified recombinant Rnt1p. The same conclusion can be drawn for the strong cleavage defect induced by the wobble U·G and U·I variants.

Closing Base Pair Variants Do Not Strongly Affect the Substrate Secondary Structure. The strong inhibitory effects of some of the substitutions that were analyzed, in particular the U-DMA, could be explained by the inability of these substitutions to form stable base pairs. It has been shown that the presence of dimethyladenosines in RNA sequences tends to favor a shift from a duplex to a hairpin conformation, where the dimethylated nucleobase is not base paired (*27*). Accordingly, the formation of a canonical AGNN tetraloop structure might be disfavored in the U-DMA substrate due to the destabilization of the closing base pair. This hypothesis is unlikely because we showed that this substitution does not strongly inhibit binding (Figure 3 and Table 2), while it is known that perturbation of the AGNN terminal loop structures affects Rnt1p binding (*16*, *18*). Nevertheless, to investigate the effect of closing base pair substitutions on the secondary structure of the substrate, we submitted wild-type and closing base pair variant RNA substrates to RNase A probing. RNase A cleaves unpaired pyrimidines, therefore allowing us to investigate the base pairing status of the 5′-pyrimidine nucleotide of the closing base pair variants. Because of the chemical modification of the purines in many of the variant closing base pairs, we were unable to find a reagent appropriate for the direct probing of the base pairing status of the purine bases of the variants. RNase A probing of the wild-type and closing base pair variant substrates showed three major sites of accessibility, two of which are localized in the stem (b and c) and the third of which is localized in the pyrimidine nucleotide of the closing base pair (site a). The accessibility of stem nucleotides to RNase A cleavage (sites b and c) may be due to partial breathing of the RNA helix. The relative accessibility of the closing base pair variants to RNase A cleavage compared to that of the wild-type C-G base pair is shown in Table 2 (C-G value arbitrarily set to 1.0). This analysis revealed that RNase A accessibility of the closing base pair pyrimidine is comparable for all these substrates (Figure 4 and Table 2). The substrate showing the most increased accessibility to RNase A cleavage is the U·I variant, suggesting that the presence of the hypoxanthine base somehow destabilizes the base pairing. However, this result does not correlate with effects on cleavage, as the U·I substrate shows better cleavage

Table 2: Kinetic, Binding, and Probing Constants Obtained for the Different Closing Base Pair Variants

	wild-type C-G	U-A	U-2AP	U-DMA	U-DAP	U·G	U·I
V_i (min^{-1})	0.142 ± 0.003	0.035 ± 0.008	0.105 ± 0.011	~0	~0	0.019 ± 0.002	0.061 ± 0.012
fraction uncleaved (%)	40.5 ± 0.5	62.0 ± 0.5	52.9 ± 0.5	~100	~100	66.6 ± 0.8	61.0 ± 0.5
K_d (nM)	112.2 ± 24.2	169.5 ± 21.4	114.8 ± 27.9	160.3 ± 41.2	267.7 ± 73.8	137.7 ± 44.2	98.4 ± 23.7
RNase A accessibility	1.0	1.8	1.3	1.0	1.6	1.7	2.2

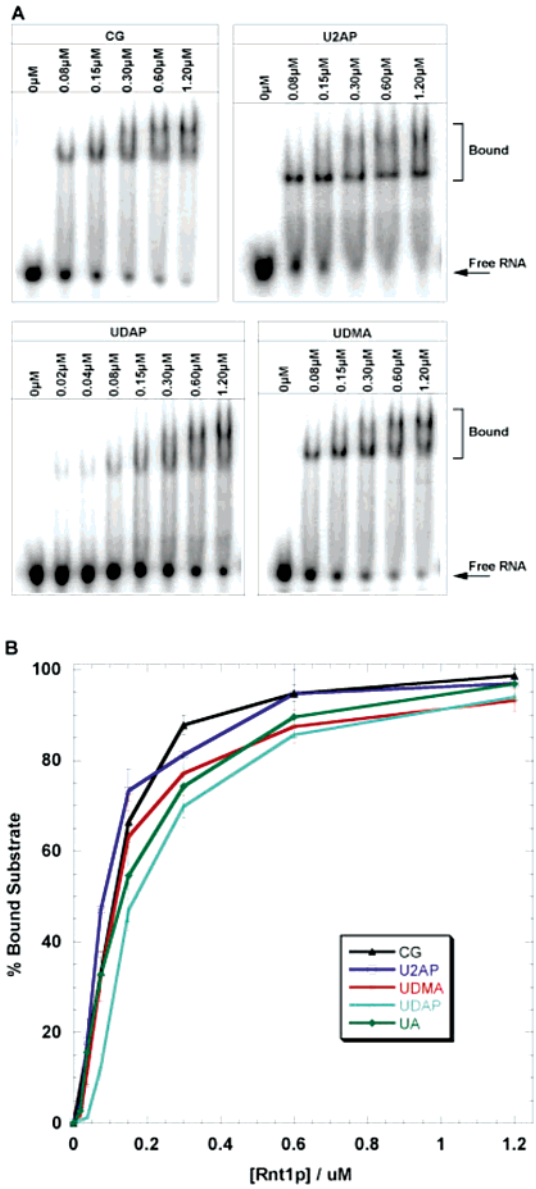

FIGURE 3: Binding of wild-type and chemically modified substrates by Rnt1p uncoupled from cleavage. (A) Shown are EMSA gels obtained with the indicated substrates and Rnt1p concentrations. The presence of multiple bands for the bound form of the RNA is consistent with dimeric and multimeric forms of Rnt1p bound to its substrate (*30*). (B) Binding curves obtained by quantification of the EMSA.

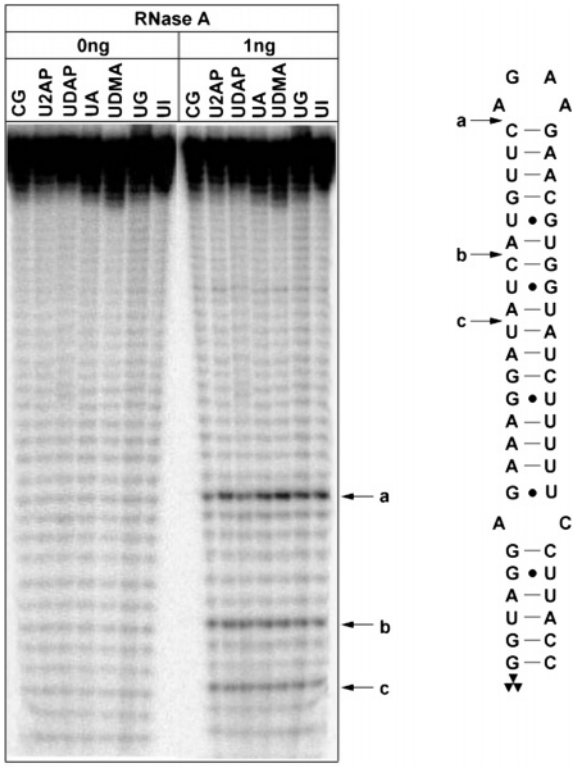

FIGURE 4: RNase A probing of the wild-type (C-G) and of the closing base pair variants used in this study. The positions of the three main cleavage sites are indicated on the secondary structure (a−c).

kinetics than the U·G substrate, which is less accessible to RNase A cleavage (Table 2). The accessibilities of the U-A and U-DAP variants were only slightly increased. The U-DMA variant exhibited the same accessibility as the wild-type C-G base pair, suggesting that the strong cleavage defect observed in this mutant cannot be attributed to a destabilization of the terminal base pair. In summary, there is no correlation between RNase A accessibility and cleavage or binding defects, suggesting that the in vitro cleavage defects observed are not due to a destabilization of the terminal base pairs in any of these variants. We also probed the structure of the AGAA tetraloop using RNase T1 cleavage, which cleaves the exposed syn guanosine in the tetraloop (*16*). We did not find any difference in RNase T1 accessibility for all the variants that were tested (data not shown), suggesting that the closing base pair variants do not strongly perturb tetraloop structure, at least at this level of analysis. Overall, these results suggest that perturbation of the base pair formation is not sufficient to explain the strong cleavage defect observed in some variants, in particular, the U-DMA substrate.

DISCUSSION

Phylogenetic analysis of RNase III substrates from *Hemiascomycetes* fungi revealed that U-A closing base pairs are almost absent from the compiled population of fungal RNase III substrates (Table 1). Subsequent biochemical analysis identified exocyclic groups located in the major groove of purines as major antideterminants at the position following the tetraloop in *Hemiascomycetes* RNase III substrates, strongly corroborating the phylogenetic observations. The most striking result is that the in vitro cleavage defect induced by a C-G to U-A mutation is almost completely suppressed by moving the adenine exocyclic

group from the major groove side to the minor groove side (U-2AP substrate). Other variants with different exocyclic groups in the major groove are poorly cleaved by Rnt1p, although they are efficiently bound. This is in contrast with mutations or modifications in the AGNN tetraloop region, which inhibit cleavage by Rnt1p, but also result in binding defects (*16*, *18*). For example, changing an AGNN-type loop into a GNRA loop results in a 5-fold binding defect for Rnt1p and for the dsRBD of Rnt1p (*16*, *18*). Previous studies have shown that perturbation of the sequence surrounding the tetraloop region inhibits Rnt1p binding (*23*). However, these experiments were performed with small substrates that are bound by Rnt1p but not cleaved. It is possible that for such small RNA hairpins, the binding defects are exacerbated. Furthermore, the significance of these mutations for cleavage activity could not be determined, as these substrates are too short to be cleaved.

The U-DMA and U-DAP substrates exhibited a complete absence of reactivity in vitro, but they are both bound relatively efficiently by Rnt1p as determined by EMSA. It is unlikely that the absence of cleavage of these two substrates results from the same molecular mechanism. One hypothesis to explain the effects observed for the U-DMA construct is that the tetraloop structure is destabilized because of a destabilization of the closing U-DMA base pair. Thermodynamic analysis of short RNA hairpins has shown that the closing base pair of RNA tetraloops is important for the stability of several tetraloops (*28*). However, this study did not include AGNN-type tetraloops, so it is impossible to know whether the same conclusion can be drawn for AGNN-type tetraloops. Dimethylation of adenine has been shown to result in the conversion of a dsRNA conformation to a loop conformation (*27*). However, we did not observe a strong destabilization of this base pair by RNase A probing, and if the closing base pair were destabilized, we would expect a destabilization of the tetraloop and therefore a strong binding defect for the U-DMA construct, which is not the case. Thus, we believe that the strong defect observed for the U-DMA substrate is due to the bulky dimethyl group that might sterically interfere with the catalytic positioning of the enzyme. In the case of the U-DAP substrate, the terminal U-DAP base pair is unlikely to significantly perturb the Watson−Crick geometry of the end of the double-stranded RNA helix. This is supported by work showing that an active ribozyme molecule could be selected carrying only uracil and diaminopurines as bases (*29*). In addition, RNase A probing results show that the perturbation of the base pair formation in the U-DAP is very unlikely. Therefore, we do not fully understand the nature of the inhibitory effect for this substrate. While a steric interference in the major groove is likely to be involved, it does not explain why this variant is a much worse substrate for Rnt1p than the U-A mutant.

Our analysis also explains the rarity of U·G base pairs observed in the substrate's phylogeny, since we show that removal of the exocyclic group of the guanine base in the U·I construct is sufficient to increase the kinetic parameters of this substrate. Thus, minor groove exocyclic groups of wobble base pairs may interfere with positioning of the dsRBD, as it has been shown that this side of the RNA substrate is bound by the dsRBD (*22*). It is tempting to speculate that some of the U·G sequences found in the natural substrates may be edited in vivo into U·I sequences, which would increase the efficiency of recognition by the enzyme. For the other base pair variants that we analyzed, and which obey Watson−Crick geometry, there is good correlation between the presence of bulky groups in the major groove of the 3′-purine base and inhibition of cleavage activity. The presence of these major groove exocyclic groups is unlikely to perturb the binding of the double-stranded RNA binding domain, as the contacts observed between the dsRBD and the tetraloop region occur on the opposite side of the RNA duplex, on the minor groove side of the RNA duplex (*22*). Thus, these modifications may affect the positioning of an additional structural element of the Rnt1p protein that recognizes the major groove side, or perturb the formation of the AGNN tetraloop structure. Any perturbation of the terminal tetraloop structure is expected to result in some binding defect. Therefore, we favor the hypothesis that these groups perturb the positioning of a protein domain of Rnt1p different from the dsRBD, possibly the catalytic domain or the N-terminal extension (*30*). This is consistent with hydroxyl radical footprinting experiments performed with the full-length protein, which showed that the entire tetraloop region is protected by the full-length protein (*21*), while the dsRBD contacts only the minor groove side and the last two nucleotides of the loop (*22*). Thus, we envision that these elements may perturb the positioning of the catalytic domain onto the RNA substrate. The precise elements of the protein that contact this area remain to be identified. Finally, this study shows that nucleic acid antideterminants participate in the recognition process of eukaryotic RNases III. Bacterial RNase III recognition also relies on sequence antideterminants (*31*). Although the details of the molecular antideterminants that are involved differ, this suggests an evolutionary convergence in the way bacterial and eukaryotic RNase III enzymes recognize their substrates.

ACKNOWLEDGMENT

We thank Amy Pandya and Pok Yang for the initial characterization of some of the chemically modified substrates and Dr. Evgeny Fadeev and Dr. My D. Sam for help with preparation of the table-of-contents graphic.

REFERENCES

1. Abou Elela, S., Igel, H., and Ares, M., Jr. (1996) RNase III cleaves eukaryotic preribosomal RNA at a U3 snoRNP-dependent site, *Cell 85*, 115−124.
2. Kufel, J., Dichtl, B., and Tollervey, D. (1999) Yeast Rnt1p is required for cleavage of the pre-ribosomal RNA in the 3′ ETS but not the 5′ ETS, *RNA 5*, 909−917.
3. Wu, H., Xu, H., Miraglia, L. J., and Crooke, S. T. (2000) Human RNase III is a 160-kDa protein involved in preribosomal RNA processing, *J. Biol. Chem. 275*, 36957−36965.
4. Bernstein, E., Caudy, A. A., Hammond, S. M., and Hannon, G. J. (2001) Role for a bidentate ribonuclease in the initiation step of RNA interference, *Nature 409*, 363−366.
5. Hutvagner, G., McLachlan, J., Pasquinelli, A. E., Balint, E., Tuschl, T., and Zamore, P. D. (2001) A cellular function for the RNA-interference enzyme Dicer in the maturation of the let-7 small temporal RNA, *Science 293*, 834−838.
6. Ketting, R. F., Fischer, S. E., Bernstein, E., Sijen, T., Hannon, G. J., and Plasterk, R. H. (2001) Dicer functions in RNA interference and in synthesis of small RNA involved in developmental timing in *C. elegans*, *Genes Dev. 15*, 2654−2659.
7. Knight, S. W., and Bass, B. L. (2001) A role for the RNase III enzyme DCR-1 in RNA interference and germ line development in *Caenorhabditis elegans*, *Science 293*, 2269−2271.

8. Lee, Y., Ahn, C., Han, J., Choi, H., Kim, J., Yim, J., Lee, J., Provost, P., Radmark, O., Kim, S., and Kim, V. N. (2003) The nuclear RNase III Drosha initiates microRNA processing, *Nature 425*, 415−419.
9. Chanfreau, G., Elela, S. A., Ares, M., Jr., and Guthrie, C. (1997) Alternative 3′-end processing of U5 snRNA by RNase III, *Genes Dev. 11*, 2741−2751.
10. Abou Elela, S., and Ares, M., Jr. (1998) Depletion of yeast RNase III blocks correct U2 3′ end formation and results in polyadenylated but functional U2 snRNA, *EMBO J. 17*, 3738−3746.
11. Seipelt, R. L., Zheng, B., Asuru, A., and Rymond, B. C. (1999) U1 snRNA is cleaved by RNase III and processed through an Sm site-dependent pathway, *Nucleic Acids Res. 27*, 587−595.
12. Allmang, C., Kufel, J., Chanfreau, G., Mitchell, P., Petfalski, E., and Tollervey, D. (1999) Functions of the exosome in rRNA, snoRNA and snRNA synthesis, *EMBO J. 18*, 5399−5410.
13. Chanfreau, G., Legrain, P., and Jacquier, A. (1998) Yeast RNase III as a key processing enzyme in small nucleolar RNAs metabolism, *J. Mol. Biol. 284*, 975−988.
14. Lee, C. Y., Lee, A., and Chanfreau, G. (2003) The roles of endonucleolytic cleavage and exonucleolytic digestion in the 5′-end processing of *S. cerevisiae* box C/D snoRNAs, *RNA 9*, 1362−1370.
15. Qu, L. H., Henras, A., Lu, Y. J., Zhou, H., Zhou, W. X., Zhu, Y. Q., Zhao, J., Henry, Y., Caizergues-Ferrer, M., and Bachellerie, J. P. (1999) Seven novel methylation guide small nucleolar RNAs are processed from a common polycistronic transcript by Rat1p and RNase III in yeast, *Mol. Cell. Biol. 19*, 1144−1158.
16. Chanfreau, G., Buckle, M., and Jacquier, A. (2000) Recognition of a conserved class of RNA tetraloops by *Saccharomyces cerevisiae* RNase III, *Proc. Natl. Acad. Sci. U.S.A. 97*, 3142−3147.
17. Chanfreau, G. (2003) Conservation of RNase III processing pathways and specificity in hemiascomycetes, *Eukaryotic Cell 2*, 901−909.
18. Nagel, R., and Ares, M., Jr. (2000) Substrate recognition by a eukaryotic RNase III: The double-stranded RNA-binding domain of Rnt1p selectively binds RNA containing a 5′-AGNN-3′ tetraloop, *RNA 6*, 1142−1156.
19. Wu, H., Yang, P. K., Butcher, S. E., Kang, S., Chanfreau, G., and Feigon, J. (2001) A novel family of RNA tetraloop structure forms the recognition site for *Saccharomyces cerevisiae* RNase III, *EMBO J. 20*, 7240−7249.
20. Lebars, I., Lamontagne, B., Yoshizawa, S., Abou-Elela, S., and Fourmy, D. (2001) Solution structure of conserved AGNN tetraloops: Insights into Rnt1p RNA processing, *EMBO J. 20*, 7250−7258.
21. Lamontagne, B., and Elela, S. A. (2004) Evaluation of the RNA determinants for bacterial and yeast RNase III binding and cleavage, *J. Biol. Chem. 279*, 2231−2241.
22. Wu, H., Henras, A., Chanfreau, G., and Feigon, J. (2004) Structural basis for recognition of the AGNN tetraloop RNA fold by the double-stranded RNA-binding domain of Rnt1p RNase III, *Proc. Natl. Acad. Sci. U.S.A. 101*, 8307−8312.
23. Lamontagne, B., Ghazal, G., Lebars, I., Yoshizawa, S., Fourmy, D., and Elela, S. A. (2003) Sequence dependence of substrate recognition and cleavage by yeast RNase III, *J. Mol. Biol. 327*, 985−1000.
24. Zuker, M. (2003) Mfold web server for nucleic acid folding and hybridization prediction, *Nucleic Acids Res. 31*, 3406−3415.
25. Danin-Kreiselman, M., Lee, C. Y., and Chanfreau, G. (2003) RNAse III-mediated degradation of unspliced pre-mRNAs and lariat introns, *Mol. Cell 11*, 1279−1289.
26. Lamontagne, B., and Elela, S. A. (2001) Purification and characterization of *Saccharomyces cerevisiae* Rnt1p nuclease, *Methods Enzymol. 342*, 159−167.
27. Micura, R., Pils, W., Hobartner, C., Grubmayr, K., Ebert, M. O., and Jaun, B. (2001) Methylation of the nucleobases in RNA oligonucleotides mediates duplex-hairpin conversion, *Nucleic Acids Res. 29*, 3997−4005.
28. Antao, V. P., and Tinoco, I., Jr. (1992) Thermodynamic parameters for loop formation in RNA and DNA hairpin tetraloops, *Nucleic Acids Res. 20*, 819−824.
29. Reader, J. S., and Joyce, G. F. (2002) A ribozyme composed of only two different nucleotides, *Nature 420*, 841−844.
30. Lamontagne, B., Tremblay, A., and Abou Elela, S. (2000) The N-terminal domain that distinguishes yeast from bacterial RNase III contains a dimerization signal required for efficient double-stranded RNA cleavage, *Mol. Cell. Biol. 20*, 1104−1115.
31. Zhang, K., and Nicholson, A. W. (1997) Regulation of ribonuclease III processing by double-helical sequence antideterminants, *Proc. Natl. Acad. Sci. U.S.A. 94*, 13437−13441.

BI047483U